Numerical Analysis of Floating-Body Motions in Arbitrary Bathymetric Domain

Taeyoung Kim, Yonghwan Kim*
Department of Naval Architecture and Ocean Engineering, Seoul National University
1, Gwanak-ro, Gwanak-gu, Seoul, Korea, (* yhwankim@snu.ac.kr)

1. INTRODUCTION

Recently, the installation of floating-type offshore structures in coastal area has been seriously considered. These offshore structures have drafts over 10 meters, and thus the shallowest conditions for operation are nearly 15~30 meters depth. For such finite water depth, the effect of bottom topology may be predominant to the wave propagation and motion responses of floating body.
One of concerns for finite depth is the nonlinear effect due to finite depth. To observe such effect, computational results based on the Boussinesq equation and Rankine panel method are compared for various bathymetry. The nonlinear solutions are obtained by the Boussinesq equation solver, while the Rankine panel method is applied for linear problems. The comparison is made for the two sets of computational result: wave propagation and wave-induced motion responses. In the both cases, the Boussinesq model does not show significantly different results from linear theory as long as water depth is not very shallow. Therefore, it can be found that a linear approach is useful for evaluating seakeeping performance of floating bodies in finite depth. Based on the linear regime, the motions responses of an LNG carrier at a port in Korea are computed.

2. BACKGROUND

2.1. Rankine Panel Method for Linear Problems

Laplace equation and linearized boundary conditions are applied to solve the boundary conditions for wave-body interaction. When sea bottom varies, the general solutions of incident waves, ϕI and ζI, are hard to find. In order to simulate incident wave adequately, wave making wall is implemented in incoming boundary surface (see Fig.1). Neumann-type boundary condition is applied at this boundary, as in Eq. (1). Furthermore, numerical damping zone is adopted on free surface, as in Eq (2), and the damping intensity, ν, is modified according to its proper behavior at the end of the computation domain.

$$\frac{\partial\phi}{\partial n}=\frac{\partial\phi_I}{\partial n} \tag{1}$$

$$\frac{d\zeta}{dt}=\frac{\partial\phi}{\partial z}-2\nu(\zeta-\zeta_I)+\frac{\nu^2}{g}(\phi-\phi_I) \tag{2}$$

Rankine sources are distributed at boundary surfaces including sea bottom. Green's second identity can be used to compute the velocity potential, ϕ, as in Eq. (3). S_F, S_B, S_{BT} denote free surface, body, and bottom, respectively. All physical values are presented by applying bi-quadratic spline basis function.

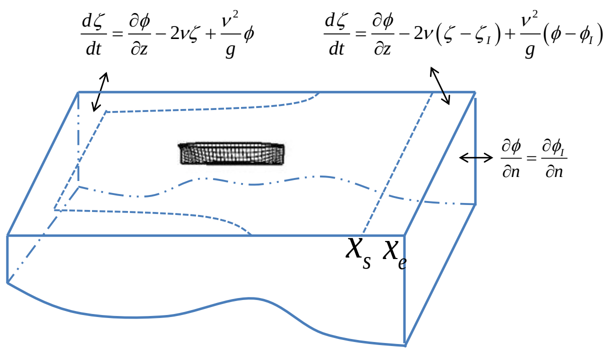

Fig. 1 Coordinate system

$$\phi+\iint_{S_F}\phi\frac{\partial}{\partial n}\left(\frac{1}{r}\right)ds+\iint_{S_B}\frac{1}{r}\frac{\partial\phi}{\partial n}ds+\iint_{S_{BT}}\frac{1}{r}\frac{\partial\phi}{\partial n}ds=\iint_{S_F}\frac{1}{r}\frac{\partial\phi}{\partial n}ds+\iint_{S_B}\phi\frac{\partial}{\partial n}\left(\frac{1}{r}\right)ds+\iint_{S_{BT}}\phi\frac{\partial}{\partial n}\left(\frac{1}{r}\right)ds \tag{3}$$

This Rankine panel method is applied in time domain to solve the prescribed boundary value problems. Wave loads are computed by integrating pressure on mean body, which is computed from Bernoulli equation. The fourth-order predictor-corrector method is applied for updating velocity potential and wave elevation. Radiation condition at far field is satisfied by applying damping zone, as similarly in Eq. (2).

2.2. Boussinesq Equation for Nonlinear Problems

Boussinesq equation approximates the velocities in fluid as a series form expanded from a reference location. In the present study, one of the state-of-the-art research is adopted which is developed by Madsen et al. (2006).

In this approach, the horizontal and vertical velocity of fluid can be represented as a series form of pseudo velocities, $\hat{\boldsymbol{u}}^*$ and $\hat{w}^*$, as in Eqs. (4) and (5). The infinite series of partial differential operators, J_I and J_{II}, include the differentiation up to fifth order.

$$\boldsymbol{u}(x,y,z,t) = J_I\hat{\boldsymbol{u}}^* + J_{II}\hat{w}^* \quad (4)$$

$$w(x,y,z,t) = J_I\hat{w}^* - J_{II}\hat{\boldsymbol{u}}^* \quad (5)$$

Pseudo velocities are computed by solving nonlinear boundary conditions with finite difference method. Then, horizontal and vertical velocities in the fluid can be calculated from Eqs. (4) and (5). Kinematic and dynamic free surface boundary conditions can update the velocities and wave elevation, by applying time-marching method.

3. NUMERICAL RESULTS

3.1. Comparison of Linear and Nonlinear Waves, and Motion Responses

Kinematic wave shapes are compared in two different depth conditions. At first, wave elevation is simulated in constant water depth by Rankine panel method and Boussinesq model. Because the modern ships have design draft around 10 meters, water depth is considered to be 15 meters to confirm the safety of under keel clearance. Fig. 2 shows the numerically generated waves in two different wave frequencies (ω), and those are compared to analytic solution of Stokes' linear wave. Longitudinal and vertical scales are normalized by wave length and a half of targeting wave height (H), respectively. In the Boussinesq model, two different wave heights, which are denoted in normalized from by water depth h, are selected to see the effect of nonlinearity. The nonlinear results in the Boussinesq model are not different significantly from the linear solution of the Rankine panel method. In addition, the results in both models are almost overlapped to the solution of Stokes' wave.

In next stage, wave elevation is simulated in sloped bottom. Sloped bottom is a useful example to describe the general shape of ocean bottom in near shore area. Many researchers have focused the effect of sloped bottom to dynamics of floating bodies (Buchner, 2006; Ferreira and Newman, 2009; Hauteclocque et al., 2009). Two different wave slopes are assumed, as in Fig. 3. h_0 and λ_0 denote water depth and wave length in inlet region. Wave elevations in both models show reasonable agreement to each other. Nonlinear effect is not dominant even at the higher wave amplitude in the Boussinesq model.

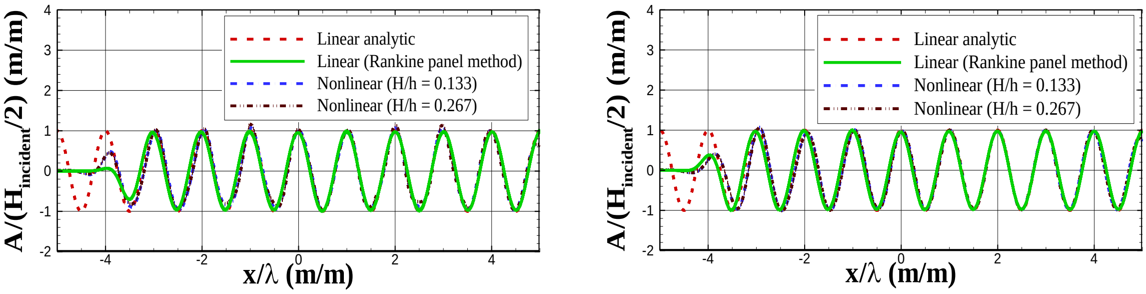

(a) Wave elevation ($\omega\sqrt{\lambda/g}=1.509$, $h/\lambda=0.060$) (b) Wave elevation ($\omega(\lambda/g)^{1/2}$=2.057, h/λ=0.130)

Fig. 2 Instantaneous wave elevation in constant water depth

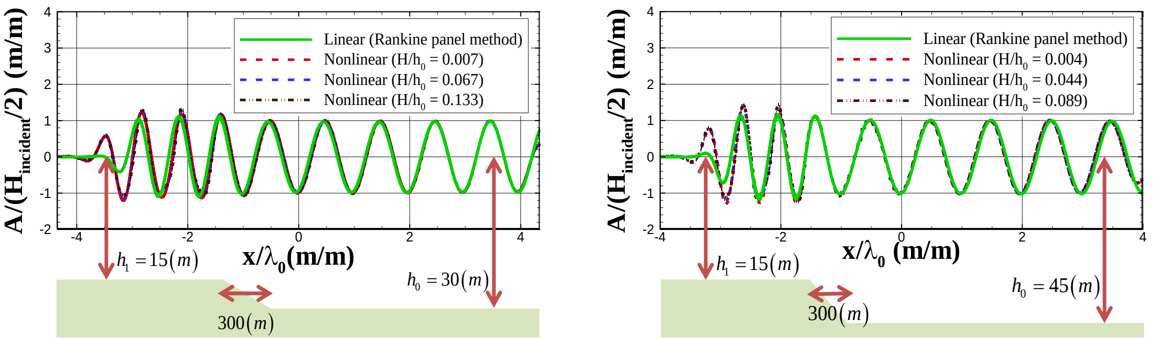

(a) Wave elevation ($\omega\sqrt{\lambda_0/g}=1.773$, $h_0/\lambda_0=0.088$) (b) Wave elevation ($\omega(\lambda_0/g)^{1/2}$=1.939, h_0/λ_0=0.110)

Fig. 3 Instantaneous wave elevation in sloped bottom

Fig.4 shows the Froude-Krylov forces computed for the sloped bottom of Fig. 3(b). In this case, the ship model is an LNG carrier of 274m length and 11m draft. The LNG carrier is assumed to be located in the center of slopes, and bow towards to deeper region. The Froude-Krylov forces are only computed in the Boussinesq model. In three different wave heights, the Froude-Krylov heave force and pitch moment are not remarkably different, as shown in Fig. 4. This results implies that the nonlinearity is not significant in this water depth.
Fig.5 shows the heave and pitch motions in two different bottom changes. Particularly, the motion RAOs are compared with those for constant depths at the middle of slopes. It is interesting that the overall trends are similar between the results.
In this computational study, it is found that nonlinear effect is not significant in the moderate water depth where coastal LNG platforms can be installed. Therefore, a linear method can be useful in the analysis of wave loads and motion responses of ships and offshore structures in finite depth.

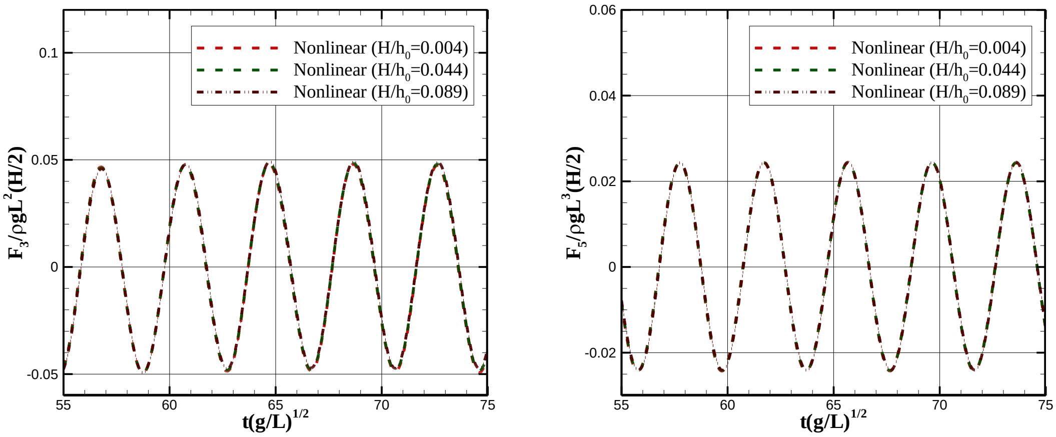

(a) Heave force (b) Pitch moment

Fig. 4 Froude-Krylov force and moment on LNG carrier (head sea, $\omega\sqrt{\lambda_0 / g} = 1.939$, $h_0 / \lambda_0 = 0.110$)

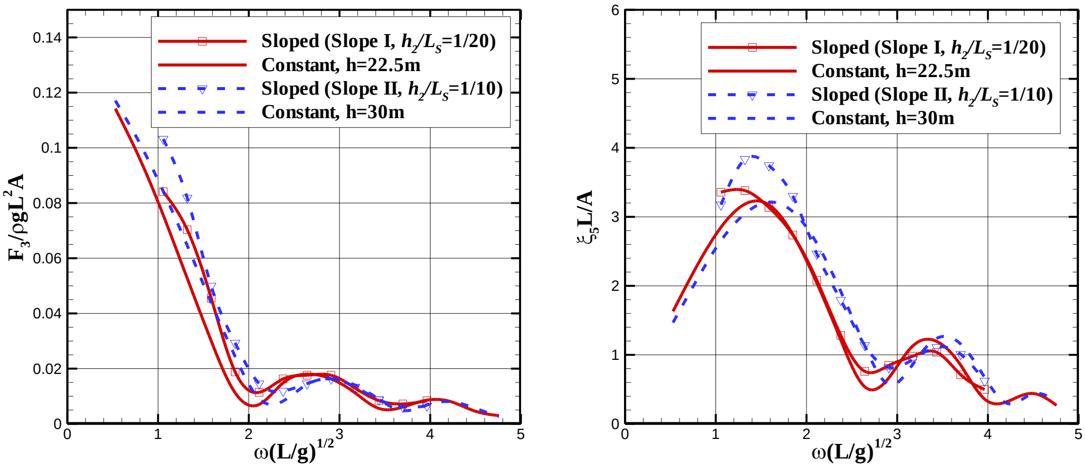

(a) Heave (b) Pitch

Fig. 5 Heave and pitch motions of LNG carrier: head sea, two bottom slopes (I: 15~30m, II: 15~45m)

3.2. Motion Responses of LNG Carrier in a Real Port

A real ocean seabed is modeled where the ship provides LNG to inland facility. The port is located at West Sea in South Korea. Fig. 6 shows the geometry around LNG terminal and representative wave flow in numerical computation. The mean depth near body is about 15 meters. Incident waves are assumed to propagate from open sea (left in figure) to narrow bay (right in figure). The direction of inflow changes due to the transversely varying bottom. In addition, the water depth also decreases as waves propagate along the bay. As a result, the shoaling effect usually increases wave amplitude in shallower region.

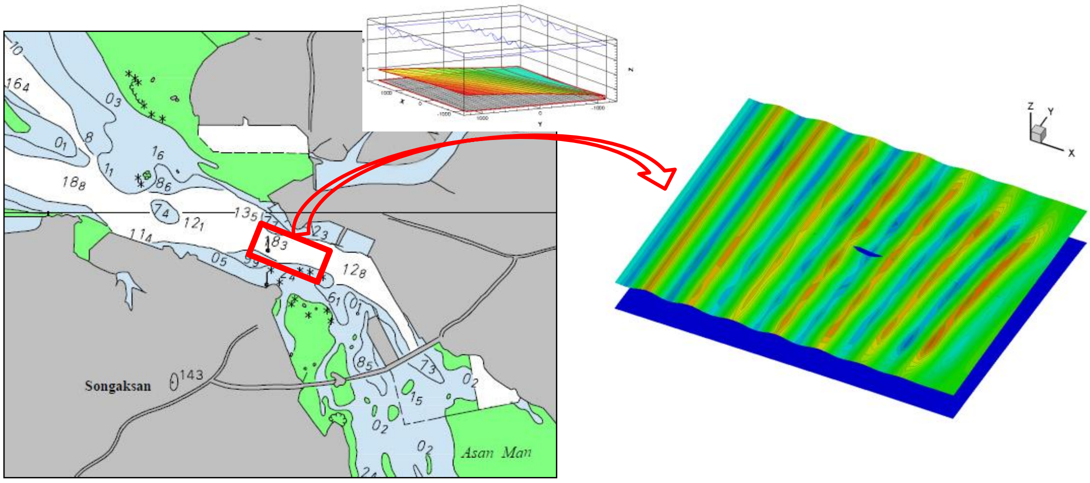

Fig. 6 Geometry of port in West Sea and representative wave around LNG carrier

Head and following waves are assumed at the inlet boundary to observe the body's responses. However, transverse flow is naturally generated due to the refraction of wave, as observed in Fig. 6. The direction is dependent on the depth variation and wave length. Fig. 7 shows the motion RAOs of the LNG carrier in regular wave. The magnitude of motion is normalized by amplitude of incident wave at inlet region. In this application, it is found that surge and heave responses are almost similar in both of head and following conditions. For pitch, the asymmetry of body and refracted waves around bow and stern regions cause different responses between head and following waves. To prevent transverse motion, position control is required according to the dominant wave component and its incident angle.

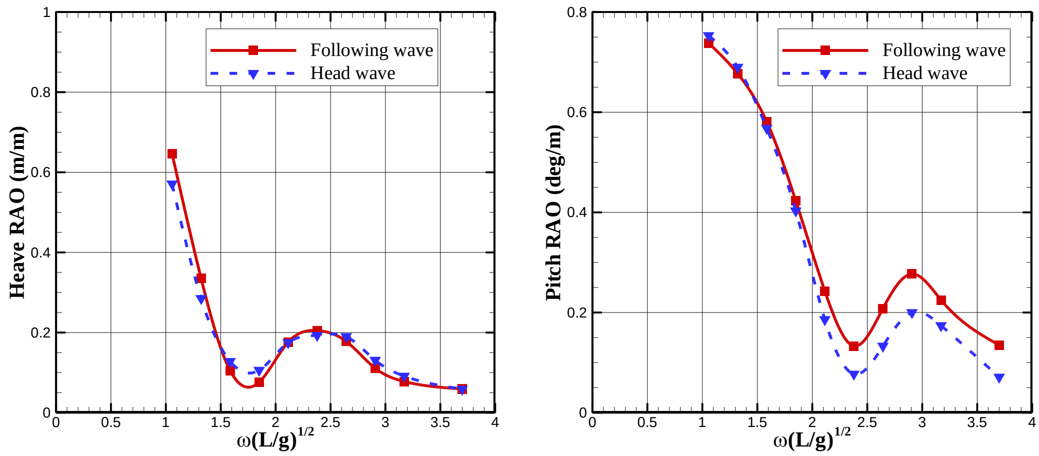

(a) Heave (b) Pitch

Fig. 7 Motion RAOs of LNG carrier around LNG terminal

REFERENCES

Belibassakis, K.A., 2008. , A boundary element method for the hydrodynamic analysis of floating bodies in variable bathymetry regions, Engineering Analysis with Boundary Elements, 32, 796– 810.

Buchner, B., 2006. The motions of a ship on a sloped seabed. In: Proceedings of 25th International Conference of Offshore Mechanics and Arctic Engineering. Hamburg, Germany.

Ferreira, MD., and Newman, JN., 2009. Diffraction effects and ship motions on an artificial seabed. In: Proceedings of 24th International Workshop on Water Waves and Floating Bodies. Zelenogorsk, Russia.

Hauteclocque, G., Rezende, F., Giorgiutti, Y., Chen, XB., 2009. Wave kinematics and seakeeping calculation with varying bathymetry. In: Proceedings of 28th International Conference of Offshore Mechanics and Arctic Engineering. Hawaii, USA.

Madsen, P., Fuhrman, R., Wang, B., 2006. A Boussinesq-type method for fully nonlinear waves interacting with a rapidly varying bathymetry. Coastal Eng. 53, 487-504.

Molin, B., Kimmoun, O., Remy, F. 2011, Slow-drift excitation in varying bathymetry, 26th IWWWFB, Athens, Greece.